

# Mitigating Noise Detriment in Differentially Private Federated Learning with Model Pre-training

Huitong Jin, Yipeng Zhou, Laizhong Cui, Quan Z. Sheng

## Abstract

Pre-training exploits public datasets to pre-train an advanced machine learning model, so that the model can be easily tuned to adapt to various downstream tasks. Pre-training has been extensively explored to mitigate computation and communication resource consumption. Inspired by these advantages, we are the first to explore how model pre-training can mitigate noise detriment in differentially private federated learning (DPFL). DPFL is upgraded from federated learning (FL), the de-facto standard for privacy preservation when training the model across multiple clients owning private data. DPFL introduces differentially private (DP) noises to obfuscate model gradients exposed in FL, which however can considerably impair model accuracy. In our work, we compare head fine-tuning (HT) and full fine-tuning (FT), which are based on pre-training, with scratch training (ST) in DPFL through a comprehensive empirical study. Our experiments tune pre-trained models (obtained by pre-training on ImageNet-1K) with CIFAR-10, CHMNIST and Fashion-MNIST (FMNIST) datasets, respectively. The results demonstrate that HT and FT can significantly mitigate noise influence by diminishing gradient exposure times. In particular, HT outperforms FT when the privacy budget is tight or the model size is large. Visualization and explanation study further substantiates our findings. Our pioneering study introduces a new perspective on enhancing DPFL and expanding its practical applications.

## Introduction

Model pre-training is an emerging technique used in machine learning (ML), where an advanced model is first trained on public datasets to learn general features and patterns before being fine-tuned on smaller, task-specific datasets (Donahue et al. 2014; He, Girshick, and Dollár 2019). This approach leverages the broad knowledge acquired during pre-training to improve performance on specific tasks (Kumar et al. 2022; Chen et al. 2020; Hendrycks, Lee, and Mazeika 2019; Junlan 2024).

Pre-training has been extensively explored for alleviating computation and communication cost in federated learning (FL). For instance, (Nguyen et al. 2023) studied how pre-trained parameters can accelerate the convergence of FL and address challenges posed by system heterogeneity.

(Chen et al. 2023) demonstrated that pre-trained parameters can narrow the performance gap between FL and centralized learning. (Sun et al. 2022) proposed a strategy of using efficient fine-tuning of pre-trained parameters to coordinate communication constraints in FL.

Despite numerous efforts dedicated to improving model training with pre-trained parameters, little effort has contributed to alleviating differentially private (DP) noise influence in FL. (Li et al. 2022b) studied that pre-training on public data can overcome the curse of dimensionality drawback in privacy-preserving ML. (Ganesh et al. 2023) demonstrated that pre-training helps the private model select a good basin in the loss landscape. (Ke et al. 2024) initially investigated the boost provided by pre-training under varying DP noise scales in ML. In view of the success of pre-training in ML, we investigate how to exploit pre-training for mitigating noise influence in differentially private federated learning (DPFL). The intuition why pre-training can enhance DPFL is briefly sketched as follows.

On the one hand, the noise scale of DPFL is amplified by exposure times (Wei et al. 2020, 2021), making advanced model training difficult. DPFL is upgraded from FL, which is the de-facto standard privacy preservation framework for model training across multiple clients. FL is conducted via multiple rounds. In each round, a coordinating server periodically exchanges gradients with clients (McMahan et al. 2017). However, exposing clients' gradients is susceptible to membership inference attacks (MIA) (Gao et al. 2023; Li, Li, and Ribeiro 2023; Liu et al. 2024) and source inference attacks (SIA) (Hu et al. 2024; Zheng and Li 2024). To defend against these attacks, DPFL introduces zero-mean noises with the scale determined by exposure times (Wei et al. 2020). If gradients are excessively exposed, the large noise scale will considerably deteriorate model accuracy.

On the other hand, the number of iteration times, *i.e.*, exposure times, of FL is heavily dependent on initial parameter values (Chen et al. 2023). Starting from pre-trained parameters, the number of exposure times of FL can be greatly prohibited, hence diminishing the DP noise scale.

In this study, we empirically examine the enhancements in DPFL achieved through pre-training. Specifically, using parameters pre-trained on ImageNet-1K (Russakovsky et al. 2015), we perform full fine-tuning (FT) and head fine-tuning (HT) on CIFAR-10 (Li et al. 2022a), CHMNIST (Kather

et al. 2016), and Fashion-MNIST (FMNIST) (Zhou et al. 2023a) datasets. In comparison, scratch training (ST) with randomly initialized parameters is also implemented. Given a certain privacy budget, the noise scale is set according to the DP mechanism, the tuned model size, iteration times, etc. Other than comparing model accuracy, we also conduct a visualization and explanation study to further substantiate our findings.

The experimental results manifest that our contribution is three-fold. *Firstly*, pre-training can significantly improve model accuracy in DPFL, striking a better trade-off between model accuracy and privacy preservation. *Secondly*, we demonstrate that HT more significantly outperforms FT when the privacy budget is tight or the model size is large. *Lastly*, we conduct the visualization study, attempting to explain the reason why pre-training enhances DPFL.

## Related Work

### Federated Learning and Differentially Private Federated Learning

FL is a distributed machine learning approach to enhancing privacy preservation (McMahan et al. 2017). Previous works have been devoted to solving the data and system heterogeneity problems in FL for accelerating the convergence rate (Wang et al. 2020; Chen et al. 2024). DPFL further enhances FL with theoretical guarantees for the privacy protection by adding random noises (Geyer, Klein, and Nabi 2017; Wei et al. 2020; Truex et al. 2020). Since original gradients are perturbed by noises, privacy is further protected with the cost of compromised model utility. To mitigate the adverse effect of noises, (Chen, Cao, and Ge 2024) enhanced privacy protection by locally adding noises and randomly shuffling the data. (Zhou et al. 2023b) optimized the number of queries and responses in DPFL for convex optimization to reduce privacy loss and improve model utility.

Nevertheless, these efforts on DPFL concentrate on noise addition mechanism design, often overlooking the importance of model initialization. To fill in this gap, we investigate the impact of initializing models with pre-trained parameters on DPFL across multiple models and datasets.

### Pre-training in Federated Learning

Pre-training in FL has garnered attention in recent studies for its potential to enhance model performance and address challenges related to system heterogeneity. (Tan et al. 2022) focused on how to effectively learn from pre-trained models, while (Sun et al. 2022) proposed the strategy to efficiently fine-tune pre-trained parameters to coordinate communication constraints in FL. (Chen et al. 2023) explored pre-training methods using synthetic data, proposing the use of fractal synthetic data to improve performance. (Nguyen et al. 2023) demonstrated that pre-trained parameters can accelerate the convergence rate of models in FL and mitigate challenges posed by system heterogeneity. However, all these studies only investigated the effects of pre-trained parameters in FL, ignoring DP. Thereby, the gain of pre-trained parameters in DPFL is still unknown.

## Privacy Attack in FL and DPFL

Even though original samples are privately retained, attackers can still attempt to recover privacy via exposed gradients such as inference attacks. Inference attacks can be broadly categorized into MIA and SIA. MIA detects if a data point was in training by analyzing model behavior differences. (Nasr, Shokri, and Houmansadr 2019) quantified privacy leakage at different layers through gradients and intermediate layer outputs. (Del Grosso et al. 2022) measured the perturbations required to construct adversarial examples. (Li, Li, and Ribeiro 2023) proposed a gradient orthogonality-based method to determine membership status without relying on shadow models or additional training. SIA focuses on identifying the source client of a specific data sample. It can perform passive attacks based on model loss information (Hu et al. 2024) or launch active attacks by poisoning the model via the server (Zheng and Li 2024).

Both MIA and SIA are attacks applicable for FL and DPFL. In this work, we implement both MIA and SIA to evaluate DPFL privacy leakage from the attack perspective under different training methods.

## Preliminaries

In this section, we introduce preliminary knowledge on DPFL and privacy attack evaluation metrics.

### Differential Privacy

DP is a rigorous privacy protection framework, originally conceived and applied in database to ensure that data is protected from malicious snooping during query processing (Dwork, Roth et al. 2014; Ma et al. 2024).

**Definition 1** ( $(\epsilon, \delta)$ -Differential Privacy): Let  $\mathcal{M}$  be a randomized algorithm. For any two datasets  $D$  and  $D'$  that differ by at most one element, and for any subset  $S$  of the output range of  $\mathcal{M}$ ,  $\mathcal{M}$  satisfies  $(\epsilon, \delta)$ -DP if:

$$\Pr[\mathcal{M}(D) \in S] \leq \exp(\epsilon) \Pr[\mathcal{M}(D') \in S] + \delta, \quad (1)$$

where  $\epsilon$  is the privacy budget and  $\delta$  is the probability of the mechanism failing to provide privacy. A smaller  $(\epsilon, \delta)$  implies a stronger level of privacy protection.

### Differentially Private Federated Learning

DPFL is upgraded from FL, which enhances client privacy protection by injecting independent and identically distributed (IID) random noises to exposed gradients (Wei et al. 2020). Suppose that there are  $N$  clients co-training the global model  $F(\theta)$ . Each client  $n \in [N]$  owns a unique training dataset  $\mathcal{D}_n$  with cardinality  $D_n$ .

DPFL is conducted via multiple global iteration rounds. In each round, DPFL obfuscates exposed sensitive gradients with noises such that attackers cannot exactly extract client privacy. In the  $t$ -th iteration, client  $n$  updates its local model using the global model  $\theta^{t-1}$  and calculates the transmitted gradients:  $\tilde{g}_n^t = \frac{1}{D_n} \sum_{i=1}^{D_n} (\text{clip}_C(g_i^t) + \mathcal{N}(0, \sigma^2))$ . Here  $g_i^t = \nabla F(\theta^{t-1}, \xi_i)$  represents the gradient for a particular sample  $\xi_i$ .  $\text{clip}_C(g_i^t) = g_i^t / \max(1, \|g_i^t\|_2 / C)$  constrains the

gradient no more than  $C$ , and  $\mathcal{N}(0, \sigma^2)$  represents Gaussian noises added to clipped gradients to ensure  $(\epsilon, \delta)$ -DP.

Note that the DP noise detriment is enlarged with respect to the total number of iterations, denoted by  $T$ . According to (Abadi et al. 2016), the noise scale is  $\sigma = c_1 q \sqrt{T \log(1/\delta)}/\epsilon$ , where  $c_1$  is a constant,  $q$  is the sampling probability. As  $T$  increases,  $\sigma$  becomes larger, which more significantly distorts the original model parameters.

After conducting local updates, the server aggregates gradients from all clients to update the global model. The aggregation process is done by averaging the updates weighted by the size of each client's dataset:  $\theta^t \leftarrow \theta^{t-1} - \eta_t \sum_{n=1}^N \frac{D_n}{D} \tilde{g}_n^t$ . Here  $D = \sum_{n=1}^N D_n$  is the size of the aggregated training set of all clients. The updated global model  $\theta^t$  is then distributed to all clients for the next iteration.

## Privacy Leakage Metrics

Although Differential Privacy (DP) offers a theoretical guarantee of privacy loss, it does not directly measure or visualize privacy leakage. Privacy attacks offer another perspective to measure privacy leakage (Nasr et al. 2023). In this work, we implement widely-used MIA and SIA to measure and visualize DPFL privacy leakage with pre-training.

**Membership Inference Attack.** According to (Li, Li, and Ribeiro 2023), MIA calculates gradient similarity based on gradient orthogonality to infer whether a particular sample is used for training.

**Definition 2 Sample Gradient Similarity:** Given a particular sample  $\xi$ , the cosine similarity between gradients derived by the sample  $\nabla F(\theta^{t-1}, \xi)$  and exposed gradients  $\tilde{g}_n^t$  (Li, Li, and Ribeiro 2023) is defined by:  $\rho(\xi, \theta_n^t) = \frac{\langle \tilde{g}_n^t, \nabla F(\theta^{t-1}, \xi) \rangle}{\|\tilde{g}_n^t\| \|\nabla F(\theta^{t-1}, \xi)\|}$ .

MIA calculates  $\rho$  for each sample with a similarity threshold to determine membership. Specially, if  $\xi$  does not contribute to  $\tilde{g}_n^t$ , its  $\rho$  should be very low. Otherwise, a high  $\rho$  implies the presence of a member in the local update. The evaluation metric of MIA is the Area Under the Curve (AUC), which quantifies the overall effectiveness of the attack in distinguishing member from non-member samples.

**Source Inference Attack.** For SIA, we implement the loss-based source inference algorithm proposed by (Hu et al. 2024). SIA calculates the loss for  $\xi$  in  $\theta_n$ , which is recovered by the server via exposed gradients. Then, the server identifies the client whose model produces the smallest loss as the source client. The expression for SIA with privacy auditing is  $\tilde{S}_i = \arg\min_{n \in \{1, 2, \dots, N\}} \ell(\theta_n, \xi)$ , where  $\ell$  is the loss evaluating a particular sample  $\xi$  on  $\theta_n$ .

The metric to evaluate SIA is the attack success rate, defined by  $ASR = \frac{1}{D} \sum_{i=1}^D \mathbb{I}(\tilde{S}_i = S_i)$ . Here,  $\tilde{S}_i$  is the inferred source client,  $S_i$  is the actual source client, and  $\mathbb{I}(\cdot)$  is the indicator that equals 1 if the argument is true and 0 otherwise. This metric calculates the proportion of correctly inferred client sources to the total number of instances, thereby quantifying the extent of privacy leakage.

---

## Algorithm 1: The DPFL with Pre-training Algorithm

---

**Require:** Number of clients  $N$ , client datasets  $\{\mathcal{D}_n\}_{n=1}^N$ , privacy budget  $\epsilon$ , iterations times  $T$ , learning rate  $\eta_0$

**Output:** Updated global model  $\theta^T$

---

```

1: ServerUpdate:
2: if fine-tuning strategy = ST then
3:   initialize  $\theta^0$  randomly
4: else if fine-tuning strategy = FT or HT then
5:   initialize  $\theta^0$  with pre-trained parameters
6: end if
7: for  $t \leftarrow 0$  to  $T - 1$  do
8:   for each client  $n \in \{N\}$  in parallel do
9:      $\tilde{g}_n^{t+1} \leftarrow \text{ClientUpdate}(\theta^t)$ 
10:   end for
11:    $\eta_t \leftarrow \eta_0 \times 0.9934^t$  and  $\theta^{t+1} \leftarrow \theta^t - \eta_t \sum_{n=1}^N \frac{D_n}{D} \tilde{g}_n^{t+1}$ 
12: end for
13:
14: ClientUpdate( $\theta^t$ ):
15:  $\theta_n^t \leftarrow \theta^t$  and  $g_n^{t+1} \leftarrow \nabla F(\theta_n^t, \mathcal{D}_n)$ 
16: if fine-tuning strategy = ST or FT then
17:    $\tilde{g}_n^{t+1} = \frac{1}{D_n} \sum_{i=1}^{D_n} (\text{clip}_C(g_i^{t+1}) + \mathcal{N}(0, \sigma^2))$ 
18: else if fine-tuning strategy = HT then
19:    $\tilde{g}_{n,head}^{t+1} = \frac{1}{D_n} \sum_{i=1}^{D_n} (\text{clip}_C(g_{i,head}^{t+1}) + \mathcal{N}(0, \sigma^2))$ 
20: end if
21: return  $\tilde{g}_n^{t+1}$ 

```

---

## Empirical Study Design

In this section, we introduce how our empirical study is designed to evaluate the gain of pre-training in DPFL.

### Training Strategies and DPFL Framework

To investigate the gain brought by pre-training, we implement three kinds of training strategies.

**Scratch Training (ST):** For DPFL with ST, the global model  $\theta^0$  is randomly initialized. ST is the baseline, based on which we can gauge the gain brought by pre-training.

**Full Fine-tuning (FT):** In FT,  $\theta^0$  is obtained by training the model on ImageNet-1K. FT will further tune all layers of the pre-trained model in DPFL with the target dataset.

**Head Fine-tuning (HT):** In HT,  $\theta^0$  is obtained in the same way as FT. However, HT only fine-tunes the final layer or head of the pre-trained model by freezing the rest parameters. Here, we suppose that the DPFL task is to train a classifier. Compared with FT, HT only exposes a much smaller fraction of gradients since most parameters are frozen, potentially reducing noise influence.

To be rigorous, let  $\theta_{head}^t$  and  $\theta_{body}^t$  denote the parameters of the classifier head and the feature extractor, respectively. During HT in DPFL, the feature extractor  $\theta_{body}^t$  is frozen, while  $\theta_{head}^t = \theta_{head}^{t-1} - \eta_t \sum_{n=1}^N \frac{D_n}{D} \tilde{g}_{n,head}^t$ .

All three training methods can be unified in the DPFL framework as presented in Algorithm 1.

### Empirical Study Cases Design

We proceed to elaborate the design of our experiments under various scenarios.

**Case 1: Broad Test.** DPFL is a generic framework that can be executed under various scenarios. We design experiments to evaluate whether pre-training can broadly improve DPFL performance under diverse scenarios. More specifically, we implement the ResNet20 model (He et al. 2016). The amount of privacy budget consumed by each client is fixed in advance. Then, we compare three training strategies by varying the system scale  $N$ , the heterogeneity degree of data distribution on clients, and the hyper-parameter  $T$ .

Through Case 1, we demonstrate that 1) pre-training can broadly improve model accuracy of DPFL under various scenarios with fixed privacy budget consumption, and 2) the gain of pre-training is sensitive to the hyper-parameter  $T$ , which should be tuned properly.

**Case 2: Extreme Test.** In this case, we consider extreme test experiments with increasing model size (denoted by  $d$ ) and the decreasing privacy budget. According to (Abadi et al. 2016), the cumulative noise scale across  $d$  model dimensions is inflated with the increase of  $d$  or the decrease of the privacy budget. More specifically, the privacy budget ( $\epsilon$ ) for each client gradually diminishes from a lenient 9.0 to a stringent 1.0, while the model scale is increased from a simple CNN model with about 0.5M parameters to the ResNet34 model with around 21M parameters (with details presented in Table 1). Under these settings, we compare the performance of different training strategies, aiming to identify the best strategy under extreme test experiments.

**Case 3: Visualization and Explanation.** Furthermore, we visualize the privacy leakage of each training strategy by evaluating privacy attack performance and displaying noise variances. The visualization study not only confirms the advantages of pre-training compared to ST but also explains why FT and HT can outperform ST in DPFL. In this case, note that we conduct MIA and SIA independently based on exposed gradients in each iteration, and output the best attack performance over the entire learning process.

## Experiments

### Experiment Setup

**Data and Model.** We conduct comprehensive experiments pertaining to visual recognition tasks. To evaluate the impact of pre-trained parameters on mitigating the influence of DP noises, we utilize three benchmark datasets: CIFAR-10 (Li et al. 2022a), CHMNIST (Kather et al. 2016), and FMNIST (Zhou et al. 2023a). For backbone, we use ResNet20 (He et al. 2016) by default, motivated by its widespread use and proven effectiveness in various visual recognition tasks.

We consider three strategies for model initialization: ST, FT and HT. For FT and HT, pre-trained parameters are obtained by using the ImageNet-1K dataset.

**Hyper-parameter Setup.** In our experiments, by default we set the number of clients participating in DPFL to  $N = 10$ , and set the number of local iterations conducted on clients to 1 per global iteration, set the local batch size to  $D_n$ , according to the standard FedSGD setting (McMahan et al. 2017). We employ the Dirichlet distribution, following (Hsu,

	CNN	ResNet20	ResNet18	ResNet34
ST / FT	0.55 M	1.09 M	11.18 M	21.29 M
HT	1.29 K	1.29 K	5.13 K	5.13 K

Table 1: # of parameters tuned with different model sizes

Qi, and Brown 2019), to distribute data samples to clients in a non-IID manner. The Dirichlet distribution controls the non-IID degree, *i.e.*, data heterogeneity, by varying its parameter  $\alpha$ , which is set to 1.0 by default. The initial learning rate is set to  $\eta_0 = 0.6$  for CIFAR-10, 0.3 for CHMNIST, and 2.0 for FMNIST, respectively, decreasing according to  $\eta_t = \eta_0 \times 0.9934^t$ . By default, we set  $T$  to 128 global iterations, the privacy budget to  $\epsilon = 5.0$ ,  $\delta = 1e - 5$  per client, and the clipping value  $C = 10.0$ . For SIA and MIA attacks, 500 data samples are randomly selected from each client’s local dataset, forming a member dataset of 5,000 samples. Additionally, 5,000 instances selected from the test dataset serve as the non-member dataset for conducting attacks.

### Pre-training Broad Test in DPFL

**Convergence Acceleration.** It is known that pre-training can accelerate convergence in FL. In Fig. 1(a), we compare the convergence w/o pre-training to observe how pre-training accelerates DPFL convergence. As shown in Fig. 1(a), HT and FT exhibit superb performance compared to ST with or without DP noises. The results indicate that pre-trained parameters can achieve better model accuracy in fewer training rounds. Moreover, distorted by DP noises, although all strategies experience a decrease in model utility, HT suffers the least reduction. Notably, while FT initially converges faster than HT in DPFL, HT surpasses FT after around 40 training rounds because FT, by exposing more gradients, suffers more severe noise influence. It suggests that HT is less susceptible to the detrimental influence of DP noises.

**Robustness of Pre-training Gain.** To evaluate the gain of pre-training in typical FL environment, we vary the system scale  $N$  from 10 to 60 and the non-IID degree  $\alpha$  from 0.5 to 3.0. The results are presented in Figs. 1(b) and 1(c), which consistently demonstrate that HT and FT outperform ST under all these scenarios. In particular, HT shows a remarkable advantage in improving model accuracy as  $N$  increases or  $\alpha$  decreases. It highlights the robustness of HT in diverse FL scenarios, making it the optimal choice for improving model utility in DPFL. This observation is different from previous studies in FL because the DP noise influence is absent from these study. The noise influence on FT is more severe because FT exposes much more gradients than HT, and consequently HT outperforms FT in DPFL.

**Critical Hyper-parameter.** According to (Abadi et al. 2016), the noise scale  $\sigma = c_1 q \sqrt{T \log(1/\delta)} / \epsilon$  increases with  $T$ . Thereby,  $T$  is a critical hyper-parameter determining the noise scale. We conduct experiments to show that the gain of pre-training is heavily subject to  $T$ , implying the importance to properly tune  $T$ .

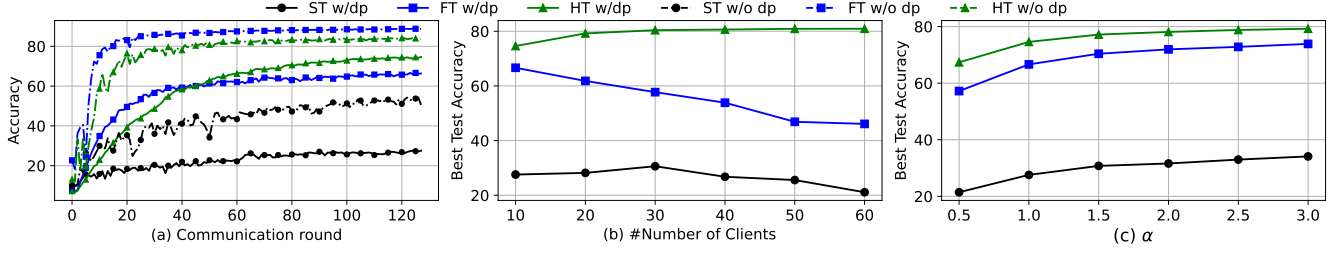


Figure 1: Comparison of model initialization across DP-FL settings. The experiments were conducted using ResNet20 on the CIFAR-10 dataset. (a) Test accuracy variation during training. (b) Best test accuracy comparison under different numbers of clients. (c) Best accuracy comparison under different degrees of data heterogeneity.

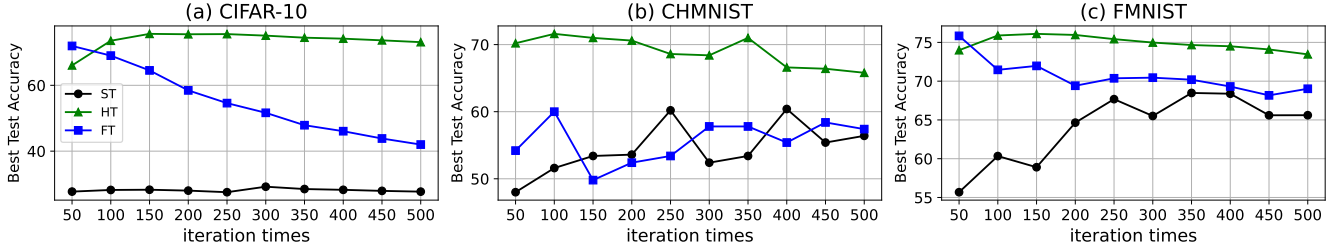


Figure 2: Impact of global iteration times on model performance across different datasets. The experiments were conducted using ResNet20 on three datasets: (a) CIFAR-10, (b) CHMNIST, and (c) FMNIST.

In Fig. 2, we compare the best model accuracy of HT, FT and ST by varying  $T$  from 50 to 500 with fixed  $\epsilon = 5.0$ . The results indicate that: 1) The improvement of pre-trained parameters is sensitive to  $T$ . For example, if we set  $T = 500$  for FT, its improvement compared to ST is very marginal. 2) The optimal  $T$  for FT is much smaller than that for HT because FT tunes much more parameters than HT per round. If  $T$  is too large for FT, the noise scale becomes too large, resulting in lowered model accuracy. 3) For all cases, HT is always the best strategy. Besides, the performance of HT is not very sensitive to  $T$ , making it much easier to tune  $T$ .

### Pre-training Extreme Test in DPFL

**Stringent Privacy Requirement with Small  $\epsilon$ .** In DPFL,  $\epsilon$  is determined by clients' privacy requirement. It is challenging to train the global model if clients have stringent privacy requirement (with a very small  $\epsilon$ ). We vary  $\epsilon$  from 1 to 9 to observe how FT and HT can improve DPFL under extreme scenarios with stringent privacy requirement.

We conduct experiments by using three datasets: CIFAR-10, CHMNIST, and FMNIST. As shown in Fig. 3, we can draw the following observations: 1) The decrease of  $\epsilon$  dilates the noise scale, thereby degrading model performance. 2) When  $\epsilon$  is extremely small, the gain of HT is more significant because HT only tunes the last layer parameters by freezing body parameters, implying that only the last layer parameters are influenced by noises. 3) When  $\epsilon$  is very small, the accuracy of FT is even worse than that of ST. The reason is that FT commences parameter tuning from a pre-trained dataset, making it difficult to find a better local optimum in the target dataset under large noises. 4) However, when  $\epsilon$

is large, FT can outperform HT, which can be intuitively explained as follows. With the increase of  $\epsilon$ , the environment of DPFL gets closer to that of FL. The influence of noises diminishes. When  $\epsilon$  exceeds a certain value, FT tuning all parameters can finally achieve better performance. If  $\epsilon = +\infty$ , it becomes equivalent to FL, in which previous studies (Nguyen et al. 2023; Sun et al. 2022) have demonstrated that FT outperforms HT.

**Large Model Size.** The trend is that the model size (denoted by  $d$ ) is getting larger. Since DP independently distorts each model dimension, a larger  $d$  in DPFL implies more noises and lower model accuracy.

To investigate how pre-training improves DPFL under different model sizes, we implement CNN, ResNet20, ResNet18, and ResNet34 models with detailed parameter size presented in Table 1. Table 2 compares model accuracy among HT, FT, and ST across various model sizes. Here  $\Delta_{HT-FT}$  denotes the accuracy gap between HT and FT. The results indicate that HT outperforms FT for all cases. In particular, HT improvement is more significant if the model size is larger. The reason lies in that HT only tunes the last layer parameters, which are not very sensitive with the increase of the model size  $d$ . For instance, when training the ResNet34 model, FT needs to tune a total of 21.29M parameters, whereas HT only tunes the last layer with 5.13K parameters.

### Visualization and Explanation

**Privacy Attack.** We conduct MIA and SIA based on exposed  $\tilde{g}_n^t$  in each round  $t$  to observe the actual privacy

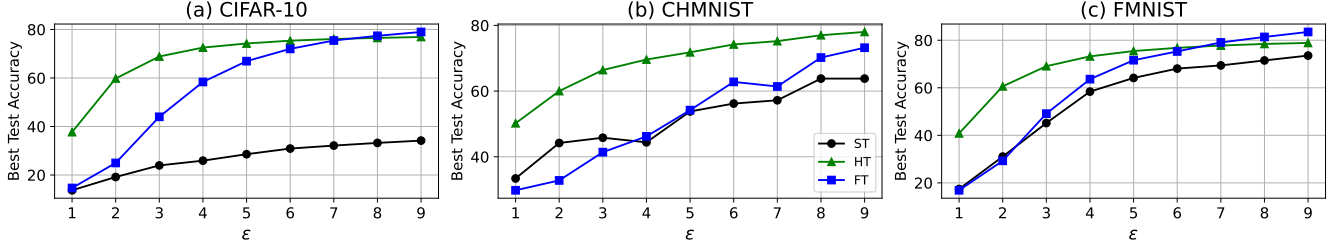


Figure 3: Impact of differential privacy budget  $\epsilon$  on model performance across different datasets. The experiments were conducted using ResNet20 on three datasets: (a) CIFAR-10, (b) CHMNIST, and (c) FMNIST.

Model	CIFAR-10				CHMNIST				FMNIST			
	ST	FT	HT	$\Delta_{HT-FT}$	ST	FT	HT	$\Delta_{HT-FT}$	ST	FT	HT	$\Delta_{HT-FT}$
CNN	33.71	45.28	53.44	8.16	53.80	56.80	69.00	12.20	74.98	74.26	73.27	-0.99
ResNet20	27.58	66.64	74.56	7.92	51.80	51.60	70.20	18.60	60.34	70.83	75.66	4.83
ResNet18	27.14	41.38	64.47	23.09	58.20	60.80	83.20	22.40	50.45	48.11	73.57	25.46
ResNet34	22.06	35.63	63.76	28.13	53.00	55.40	82.00	26.60	40.88	37.87	72.98	35.11

Table 2: Comparison of model initialization strategies based on accuracy across different model size in DPFL settings.

leakage when confronting attacks. The adopted model is ResNet20 with results presented in Fig. 4, under various privacy budgets, with other parameters set by default. The experimental results reveal that: 1) There is a trade-off between model accuracy and privacy leakage amount. FT and HT improve model accuracy of DPFL at the cost of more privacy leakage. Overall, HT is more vulnerable to attacks than FT. It is not difficult to understand this trade-off. Even in FL without DP, if the co-trained global model has very low accuracy, it will not leak much privacy as well because the model does not contain much useful knowledge learned from clients. 2) By considering the improvement of pre-training presented in Fig. 3, it is worth exploiting FT and HT in DPFL because their improvement gain far exceeds the higher privacy cost. If the privacy protection is stringent, we can calibrate the privacy budget of FT and HT, so as to avoid excessive privacy leakage. To better illustrate this point, we compare the improvement v.s. privacy leakage in Table 3 for the particular case with  $\epsilon = 3$ . Specifically, HT improves ResNet20 accuracy by 187.40%, 44.98%, and 52.97% across CIFAR-10, CHMNIST, and FMNIST, respectively. In contrast, attack performance of HT in terms of MIA AUC and SIA ASR is only moderately increased.

**Further Understanding.** We further illustrate the advantages of HT over ST and FT through a visualization study. 1) *Training Loss*: Due to domain shift (Yosinski et al. 2014; Nguyen et al. 2023) (from ImageNet-1K to CIFAR-10), initial training loss of FT and HT is higher than ST. However, Fig. 5(a) shows that parameter fine-tuning by HT and FT can converge much faster than ST because of generic features learned from pre-training. 2) *Noise Accumulation*: Let  $\tilde{\theta}_t$  and  $\theta_t$  denote global model parameters at round  $t$  for models trained w and w/o dp noises, respectively. The L2-norm distance  $\kappa_t = \|\tilde{\theta}_t - \theta_t\|_2$  quantifies the magni-

Dataset	Metric	ST	FT Inc.	HT Inc.
CIFAR-10	Accuracy	23.96	83.64%	<b>187.40%</b>
	MIA AUC	57.17	13.63%	15.62%
	SIA ASR	20.48	11.62%	22.36%
CHMNIST	Accuracy	45.80	-9.61%	<b>44.98%</b>
	MIA AUC	57.10	5.57%	12.82%
	SIA ASR	18.98	7.06%	17.97%
FMNIST	Accuracy	45.16	8.75%	<b>52.97%</b>
	MIA AUC	58.37	6.60%	14.29%
	SIA ASR	19.86	10.78%	24.57%

Table 3: Relative Metric Increase of FT and HT Compared to ST for  $\epsilon = 3.0$  on ResNet20.

tude of DP noise interference at iteration  $t$ . As shown in Fig. 5(b), for FT and ST, the cumulative DP noise influence dilates with a  $\sqrt{t}$  growth rate with iterations. In comparison, the influence on HT (which only tunes a small portion of parameters) is stable with iterations<sup>1</sup>. 3) *Gradient Similarity*: Let  $\tilde{g}_t = \frac{D_n}{D} \tilde{g}_n^t$  denote the global model update iteration  $t$ . The cosine similarity between  $\tilde{g}_t$  and  $\tilde{g}_{t-1}$ , given by  $\rho(\tilde{g}_t, \tilde{g}_{t-1}) = \frac{\tilde{g}_t \cdot \tilde{g}_{t-1}}{\|\tilde{g}_t\| \|\tilde{g}_{t-1}\|}$ , measures the consistency of model update directions between consecutive iterations. Note that  $\tilde{g}_n^t$  should be replaced by  $\tilde{g}_{n,head}^t$  when calculating  $\rho$  for HT. As shown in Fig. 5(c), the similarity for FT and ST is nearly orthogonal, suggesting that FT and ST, due to noise distortion, fail to consistently update gradients across iterations. In contrast, for HT, the similarity deviates from zero, indicating that HT can still effectively update model

<sup>1</sup>Note that the influence on FT and ST is not identical because the effect of gradient clipping operation on FT and ST is different.



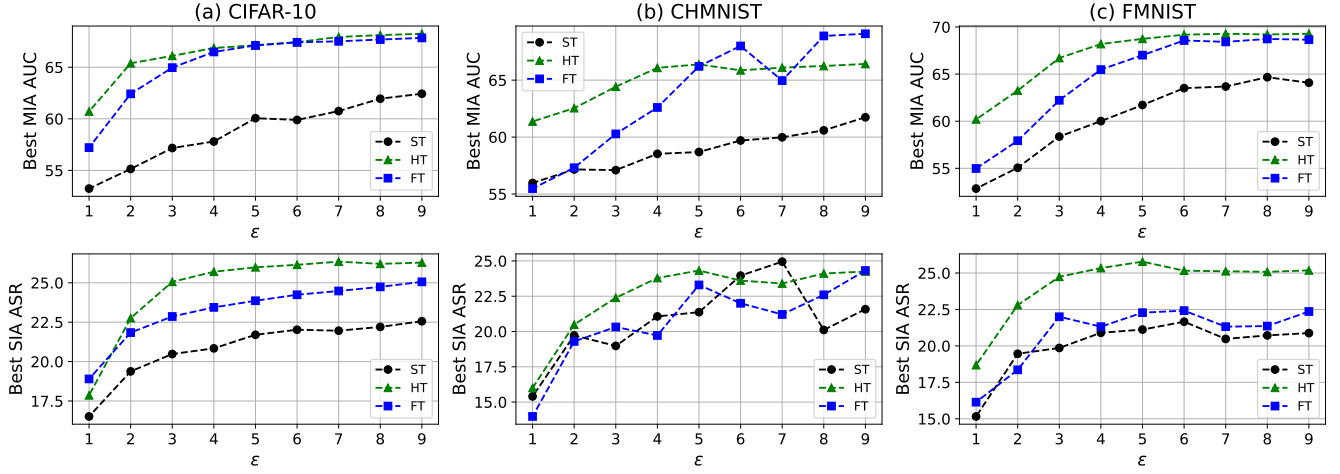


Figure 4: Impact of differential privacy budget  $\epsilon$  on privacy leakage metrics across different datasets. The first row shows the results for MIA, and the second row displays the results for SIA.

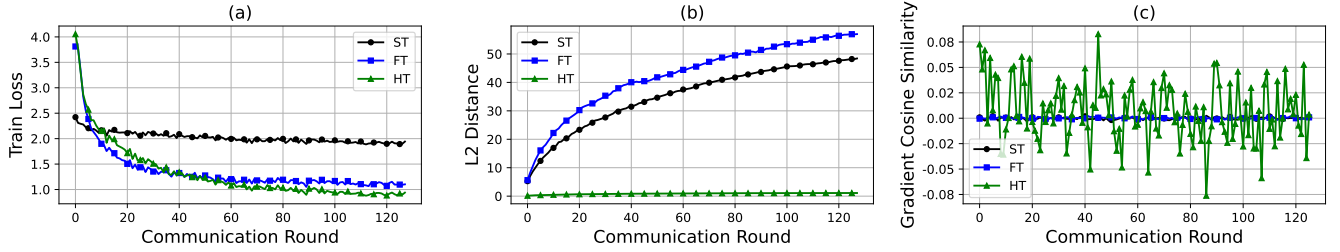


Figure 5: Understanding the role of pre-training in DPFL using ResNet20 on CIFAR-10. (a) Training loss in DPFL; (b) Distance between model parameters w/dp and w/o dp; (c) Cosine similarity between global model updates in adjacent iterations.

parameters even in the presence of noise distortion.

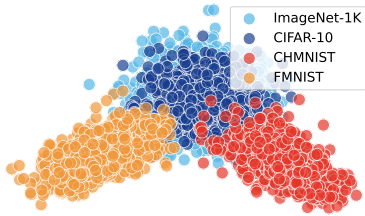


Figure 6: Data domains of different datasets in 2D space.

In Fig. 6, we explore how the domain gap (between pre-training data and target data) affects pre-training performance. We apply Linear Discriminant Analysis (LDA) method (Sun et al. 2022) to quantify and visualize the domain gap. As we can see, CIFAR-10 is the one with the smallest gap with ImageNet-1K. Meanwhile, our experimental results show that pre-training improvement is more significant on CIFAR-10 than CHMNIST and FMNIST, indicating that a smaller domain gap is more desirable.

## Conclusion and Future Work

Pre-training is known to accelerate model convergence and enhance model utility. However, the specific benefits of pre-training in DPFL and the underlying reasons remain under-explored. This work is the first to focus on improving DPFL through model pre-training, conducted via a comprehensive empirical study. By implementing and testing classical classification models on standard datasets, such as CIFAR-10, CHMNIST, and FMNIST, we demonstrate the superiority of FT and HT in the context of DPFL. Additionally, our study identifies key factors influencing the benefits of pre-training, including model size and the number of iterations. Visualization and explanation further convince our findings by conducting MIA and SIA attacks and displaying noise variation. Our work not only enhances the practicability of DP by mitigating its influence on FL, but also opens a new avenue for improving DPFL performance. We foresee future research advancing this area in three key directions: 1) Selecting or generating pre-training datasets tailored to the training task to further enhance DPFL; 2) Designing novel DP mechanisms aligned with pre-training techniques for FL; 3) Theoretical analysis of the advantages and trade-offs of pre-training concerning convergence, model accuracy, and privacy leakage in DPFL.

## References

- Abadi, M.; Chu, A.; Goodfellow, I.; McMahan, H. B.; Mironov, I.; Talwar, K.; and Zhang, L. 2016. Deep learning with differential privacy. In *Proceedings of the 2016 ACM SIGSAC Conference on Computer and Communications Security*, 308–318.
- Chen, E.; Cao, Y.; and Ge, Y. 2024. A Generalized Shuffle Framework for Privacy Amplification: Strengthening Privacy Guarantees and Enhancing Utility. In *Proceedings of the AAAI Conference on Artificial Intelligence*, volume 38, 11267–11275.
- Chen, H.; Zhang, Y.; Krompass, D.; Gu, J.; and Tresp, V. 2024. Feddat: An approach for foundation model finetuning in multi-modal heterogeneous federated learning. In *Proceedings of the AAAI Conference on Artificial Intelligence*, volume 38, 11285–11293.
- Chen, H.-Y.; Tu, C.-H.; Li, Z.; Shen, H. W.; and Chao, W.-L. 2023. On the Importance and Applicability of Pre-Training for Federated Learning. In *The Eleventh International Conference on Learning Representations, ICLR 2023, Kigali, Rwanda, May 1-5, 2023*.
- Chen, T.; Kornblith, S.; Norouzi, M.; and Hinton, G. 2020. A simple framework for contrastive learning of visual representations. In *International Conference on Machine Learning*, 1597–1607. PMLR.
- Del Grosso, G.; Jalalzai, H.; Pichler, G.; Palamidessi, C.; and Piantanida, P. 2022. Leveraging adversarial examples to quantify membership information leakage. In *Proceedings of the IEEE/CVF Conference on Computer Vision and Pattern Recognition*, 10399–10409.
- Donahue, J.; Jia, Y.; Vinyals, O.; Hoffman, J.; Zhang, N.; Tzeng, E.; and Darrell, T. 2014. Decaf: A deep convolutional activation feature for generic visual recognition. In *International Conference on Machine Learning*, 647–655. PMLR.
- Dwork, C.; Roth, A.; et al. 2014. The algorithmic foundations of differential privacy. *Foundations and Trends® in Theoretical Computer Science*, 9(3–4): 211–407.
- Ganesh, A.; Haghighi, M.; Nasr, M.; Oh, S.; Steinke, T.; Thakkar, O.; Thakurta, A. G.; and Wang, L. 2023. Why is public pretraining necessary for private model training? In *International Conference on Machine Learning*, 10611–10627. PMLR.
- Gao, J.; Jiang, X.; Zhang, H.; Yang, Y.; Dou, S.; Li, D.; Miao, D.; Deng, C.; and Zhao, C. 2023. Similarity distribution based membership inference attack on person re-identification. In *Proceedings of the AAAI Conference on Artificial Intelligence*, volume 37, 14820–14828.
- Geyer, R. C.; Klein, T.; and Nabi, M. 2017. Differentially private federated learning: A client level perspective. *arXiv preprint arXiv:1712.07557*.
- He, K.; Girshick, R.; and Dollár, P. 2019. Rethinking imagenet pre-training. In *Proceedings of the IEEE/CVF International Conference on Computer Vision*, 4918–4927.
- He, K.; Zhang, X.; Ren, S.; and Sun, J. 2016. Deep residual learning for image recognition. In *Proceedings of the IEEE Conference on Computer Vision and Pattern Recognition*, 770–778.
- Hendrycks, D.; Lee, K.; and Mazeika, M. 2019. Using pre-training can improve model robustness and uncertainty. In *International Conference on Machine Learning*, 2712–2721. PMLR.
- Hsu, H.-H.; Qi, H.; and Brown, M. 2019. Measuring the Effects of Non-Identical Data Distribution for Federated Visual Classification. *arXiv: Learning*.
- Hu, H.; Zhang, X.; Salicic, Z.; Sun, L.; Choo, K.-K. R.; and Dobbie, G. 2024. Source Inference Attacks: Beyond Membership Inference Attacks in Federated Learning. *IEEE Transactions on Dependable and Secure Computing*, 21(4): 3012–3029.
- Junlan, F. 2024. Holistic Artificial Intelligence. *Journal of Beijing University of Posts and Telecommunications*, 47(4): 1–10.
- Kather, J. N.; Weis, C.-A.; Bianconi, F.; Melchers, S. M.; Schad, L. R.; Gaiser, T.; Marx, A.; and Zöllner, F. G. 2016. Multi-class texture analysis in colorectal cancer histology. *Scientific Reports*, 6(1): 1–11.
- Ke, S.; Hou, C.; Fanti, G.; and Oh, S. 2024. On the Convergence of Differentially-Private Fine-tuning: To Linearly Probe or to Fully Fine-tune? *arXiv preprint arXiv:2402.18905*.
- Kumar, A.; Raghunathan, A.; Jones, R. M.; Ma, T.; and Liang, P. 2022. Fine-Tuning can Distort Pretrained Features and Underperform Out-of-Distribution. In *The Tenth International Conference on Learning Representations, ICLR 2022, Virtual Event, April 25-29, 2022*. OpenReview.net.
- Li, J.; Li, N.; and Ribeiro, B. 2023. Effective passive membership inference attacks in federated learning against over-parameterized models. In *The Eleventh International Conference on Learning Representations, ICLR 2023, Kigali, Rwanda, May 1-5, 2023*. OpenReview.net.
- Li, M.; Chow, S. S. M.; Hu, S.; Yan, Y.; Shen, C.; and Wang, Q. 2022a. Optimizing Privacy-Preserving Outsourced Convolutional Neural Network Predictions. *IEEE Transactions on Dependable and Secure Computing*, 19(3): 1592–1604.
- Li, X.; Liu, D.; Hashimoto, T. B.; Inan, H. A.; Kulkarni, J.; Lee, Y. T.; and Thakurta, A. G. 2022b. When Does Differentially Private Learning Not Suffer in High Dimensions? In *Advances in Neural Information Processing Systems 35: Annual Conference on Neural Information Processing Systems 2022, NeurIPS 2022, New Orleans, LA, USA, November 28 - December 9, 2022*.
- Liu, H.; Wu, Y.; Yu, Z.; and Zhang, N. 2024. Please tell me more: Privacy impact of explainability through the lens of membership inference attack. In *2024 IEEE Symposium on Security and Privacy, SP 2024*, 120–120. IEEE.
- Ma, J.; Zhou, Y.; Cui, L.; and Guo, S. 2024. An Optimized Sparse Response Mechanism for Differentially Private Federated Learning. *IEEE Transactions on Dependable and Secure Computing*, 21(4): 2285–2295.
- McMahan, B.; Moore, E.; Ramage, D.; Hampson, S.; and y Arcas, B. A. 2017. Communication-Efficient Learning



- of Deep Networks from Decentralized Data. In *Proceedings of the 20th International Conference on Artificial Intelligence and Statistics, AISTATS 2017, 20-22 April 2017, Fort Lauderdale, FL, USA*, volume 54 of *Proceedings of Machine Learning Research*, 1273–1282. PMLR.
- Nasr, M.; Hayes, J.; Steinke, T.; Balle, B.; Tramèr, F.; Jagielski, M.; Carlini, N.; and Terzis, A. 2023. Tight auditing of differentially private machine learning. In *32nd USENIX Security Symposium (USENIX Security 23)*, 1631–1648.
- Nasr, M.; Shokri, R.; and Houmansadr, A. 2019. Comprehensive Privacy Analysis of Deep Learning: Passive and Active White-box Inference Attacks against Centralized and Federated Learning. In *2019 IEEE Symposium on Security and Privacy, SP 2019, San Francisco, CA, USA, May 19-23, 2019*, 739–753. IEEE.
- Nguyen, J.; Wang, J.; Malik, K.; Sanjabi, M.; and Rabbat, M. G. 2023. Where to Begin? On the Impact of Pre-Training and Initialization in Federated Learning. In *The Eleventh International Conference on Learning Representations, ICLR 2023, Kigali, Rwanda, May 1-5, 2023*. OpenReview.net.
- Russakovsky, O.; Deng, J.; Su, H.; Krause, J.; Satheesh, S.; Ma, S.; Huang, Z.; Karpathy, A.; Khosla, A.; Bernstein, M.; et al. 2015. Imagenet large scale visual recognition challenge. *International Journal of Computer Vision*, 115: 211–252.
- Sun, G.; Mendieta, M.; Yang, T.; and Chen, C. 2022. Conquering the communication constraints to enable large pre-trained models in federated learning. *arXiv preprint arXiv:2210.01708*.
- Tan, Y.; Long, G.; Ma, J.; Liu, L.; Zhou, T.; and Jiang, J. 2022. Federated learning from pre-trained models: A contrastive learning approach. *Advances in Neural Information Processing Systems*, 35: 19332–19344.
- Truex, S.; Liu, L.; Chow, K.-H.; Gursoy, M. E.; and Wei, W. 2020. LDP-Fed: Federated learning with local differential privacy. In *Proceedings of the Third ACM International Workshop on Edge Systems, Analytics and Networking*, 61–66.
- Wang, J.; Liu, Q.; Liang, H.; Joshi, G.; and Poor, H. V. 2020. Tackling the objective inconsistency problem in heterogeneous federated optimization. *Advances in Neural Information Processing Systems*, 33: 7611–7623.
- Wei, K.; Li, J.; Ding, M.; Ma, C.; Su, H.; Zhang, B.; and Poor, H. V. 2021. User-level privacy-preserving federated learning: Analysis and performance optimization. *IEEE Transactions on Mobile Computing*, 21(9): 3388–3401.
- Wei, K.; Li, J.; Ding, M.; Ma, C.; Yang, H. H.; Farokhi, F.; Jin, S.; Quek, T. Q.; and Poor, H. V. 2020. Federated learning with differential privacy: Algorithms and performance analysis. *IEEE Transactions on Information Forensics and Security*, 15: 3454–3469.
- Yosinski, J.; Clune, J.; Bengio, Y.; and Lipson, H. 2014. How transferable are features in deep neural networks? *Advances in Neural Information Processing Systems*, 27.
- Zheng, T.; and Li, B. 2024. CMI: Client-Targeted Membership Inference in Federated Learning. *IEEE Transactions on Dependable and Secure Computing*, 21(4): 4122–4132.
- Zhou, J.; Wu, N.; Wang, Y.; Gu, S.; Cao, Z.; Dong, X.; and Choo, K.-K. R. 2023a. A Differentially Private Federated Learning Model Against Poisoning Attacks in Edge Computing. *IEEE Transactions on Dependable and Secure Computing*, 20(3): 1941–1958.
- Zhou, Y.; Liu, X.; Fu, Y.; Wu, D.; Wang, J. H.; and Yu, S. 2023b. Optimizing the numbers of queries and replies in convex federated learning with differential privacy. *IEEE Transactions on Dependable and Secure Computing*, 20(6): 4823–4837.